Eur Biophys J (1987) 15: 133–140

European Biophysics Journal

The superstructure of chromatin and its condensation mechanism

IV. Enzymatic digestion, thermal denaturation, effect of netropsin and distamycin

M. H. J. Koch*, Z. Sayers, M. C. Vega, and A. M. Michon

European Molecular Biology Laboratory, c/o DESY, Notkestrasse 85, D-2000 Hamburg 52, Federal Republic of Germany

Received January 27, 1987/Accepted in revised form May 14, 1987

Abstract. Changes in the structure of chicken erythrocyte chromatin fibres at low ionic strength resulting from enzymatic digestion, thermal denaturation and binding of Netropsin and Distamycin were monitored by synchrotron X-ray solution scattering. Digestion with micrococcal nuclease confirms the previous assignment of the 0.05 nm^{-1} band to an interference between nucleosomes with an average distance of 23 nm. The results of thermal denaturation indicate that above 40 °C there is a progressive increase of the internucleosomal distance and that above 60 °C the characteristic structure of the chromatin fibre is destroyed. Binding of Netropsin and Distamycin also results in an increase of the internucleosomal distance which can be estimated to correspond to about 0.2 nm/mol.

Key words: X-ray solution scattering, synchrotron radiation, chicken erythrocyte chromatin, rat liver chromatin, micrococcal nuclease

Introduction

During interphase most chromatin is folded into fibres with about 6 nucleosomes/11 nm length and a diameter around 30 nm. Although there is substantial agreement among the simplest models of chromatin concerning the arrangement of the nucleosomes, their connectivity, determined by the path of the linker DNA, is still undefined. This results in two types of models: the solenoid (Finch and Klug 1976) where the linker connects adjacent nucleosomes, and the crossed-linker model (Bordas et al. 1986b) where the linker connects non adjacent nucleosomes across the central part of the fibre. A number of other, more complex, models have also been described (see references in Koch et al. 1987).

The unfolded structure of chromatin, found at low ionic strength in vitro may, however, be more relevant to cellular processes, as it appears that transcription is associated with local unfolding of the 30 nm filament (for a review see Yaniv and Cereghini 1986).

X-ray solution scattering experiments are performed at chromatin concentrations, typically around $A_{260} = 70$ (3.5 mg DNA/ml), which are several orders of magnitude higher than those used in light scattering $A_{260} = 0.8$ (Ausio et al. 1984) or electric dichroism, $A_{260} = 0.2$ (Sen and Crothers 1986a). Since the DNA concentration in the nucleus can be calculated from generally accepted values of the nuclear volume and DNA content (Lewin 1980) to be of the order of 10 – 20 mg/ml, X-ray studies should provide a link between the extremes of infinite dilution and of the conditions in vivo. In previous studies (Perez-Grau et al. 1984; Bordas et al. 1986a, b; Koch et al. 1987) it was found that the X-ray solution scattering pattern of long chromatin fragments from chicken erythrocytes or rat liver at low ionic strength displays a broad maximum around $s = 0.05$ nm^{-1}. In the present paper, we show unequivocally by digestion experiments with micrococcal nuclease that this band is due to the average internucleosomal spacing in long chromatin fragments. We then use this band as a marker to monitor structural modifications in the chromatin fibre upon changes of temperature and binding of Netropsin and Distamycin (for a review see Zimmer and Wahnert 1986).

Materials and methods

Preparation of chromatin fragments

The preparation of solutions of chromatin fragments containing on average 70 to 90 nucleosomes in TE buffer (5 m*M* Tris · HCl, 1 m*M* Na_2 EDTA, 0.5 m*M* PMSF, pH 7.5) followed the procedures described ear-

* To whom offprint requests should be sent

lier (Bordas et al. 1986a). Chromatin concentrations were measured spectrophotometrically, a concentration of 1 mg chromatin/ml (0.52 mg DNA/ml) corresponding to $A_{260} = 10.4$. Unless otherwise stated final chromatin concentrations used for the X-ray solution scattering experiments were in the range 2.5 – 3 mg DNA/ml.

Digestion with micrococcal nuclease

A chromatin solution (3 mg DNA/ml) in Tris buffer was made 0.5 m*M* in Ca^{++} and digested with 15 Boehringer units/mg DNA of Micrococcal Nuclease (Sigma) for 0, 1, 2, 4, 8, 16, 32, 64 min at 37 °C. The reaction was stopped by making the solutions 2 m*M* in EDTA and cooling on ice. In control experiments, chromatin solutions with 0.5 m*M* $CaCl_2$ were left at 37 °C, without enzyme, and processed identically to the digested samples. The DNA size distribution was determined as described earlier (Koch et al. 1987) from 1% agarose gels.

Thermal denaturation of chicken erythrocyte chromatin

The thermal denaturation of CE chromatin fragments was followed by X-ray scattering with a time resolution of 60 s. The chromatin solution (3.5 mg DNA/ml) was placed in a thermostated cell connected to a water bath whose temperature was increased at a rate of about 2 °C/min from 20 °C to 90 °C.

Optical absorption measurements were performed at two different ionic conditions: in TE buffer and in the same buffer adjusted to 80 m*M* NaCl. The samples were diluted to a concentration of 0.070 mg DNA/ml. The changes in absorbance were monitored using a spectrophotometer (ZEISS DMR10). The rate of heating of the thermostated cuvette was identical to that during the X-ray experiments.

The possible degradation of histones during thermal denaturation of chromatin fragments was also investigated. A chromatin fragment sample (3.5 mg DNA/ml) in TE buffer was heated in a water bath to 70 °C at an approximate rate of 2 °C/min. An aliquot was taken at intervals of 5 °C and an acidic extraction of histones was performed as described previously (Bordas et al. 1986 a). No degradation of the histones was detected.

Binding of distamycin and netropsin

Distamycin A (Sigma) was dissolved in TE buffer and appropriate amounts of this 11 m*M* stock solution were added to chromatin solutions to obtain Distamycin/100 base pair ratios in the range 0 – 20. The concentration of chromatin varied from 2.4 to 3.4 mg DNA/ml in different experiments. In the experiments with NaCl, Distamycin was added from the stock solution to chromatin solutions in 20 m*M* or 40 m*M* NaCl.

Netropsin sulphate was kindly provided by Prof. F. Arcamone (Farmitalia Carlo Erba). A stock solution of 10 m*M* Netropsin in TE buffer was prepared and added to chromatin solutions (3.3 mg DNA/ml) in appropriate amounts to obtain Netropsin/100 base pair ratios in the range 0 – 10.

X-ray solution scattering

All experiments were performed on the double focusing monochromator mirror camera X33 (Koch and Bordas 1983) in HASYLAB on the storage ring DORIS of the Deutsches Elektronen Synchrotron (DESY) in Hamburg using a wavelength of 0.15 nm. Details of the data acquisition and evaluation systems have been given elsewhere (Boulin et al. 1982; Boulin et al. 1986). Exposure times were 3 min for all static experiments. Thermal denaturation and radiation damage were followed with a time resolution of 1 min. In order to minimize systematic errors due to small changes in the background at very low angles, care was taken to make all measurements belonging to one series as much as possible during the same injection of the storage ring. For better visualisation the experimental data are presented as plots of $\log(s\,I(s))$ vs. s, with $s = 2\sin\theta/\lambda$, where 2θ is the scattering angle and λ the wavelength.

Results

Micrococcal nuclease digestion

As illustrated in Fig. 1 A digestion with micrococcal nuclease results in a progressive decrease of the interference band at 0.05 nm^{-1}. Under the conditions used, a significant decrease of the apparent radius of gyration of the cross-section and mass per unit length occur after about 8 min and the interference band vanishes after 32 min digestion. After 64 min digestion the scattering pattern at low angles shows the presence of aggregated material probably due to digestion of the nucleosome cores and subsequent release of histones. This becomes even more evident at longer digestion times (not shown). The slope of the outer part of the cross-section plot remains constant at 3.2 ± 0.2 nm. The scattering pattern of the control samples processed in the same manner as in the digestion experiment but in absence of enzyme, were identical to that of the original undigested sample.

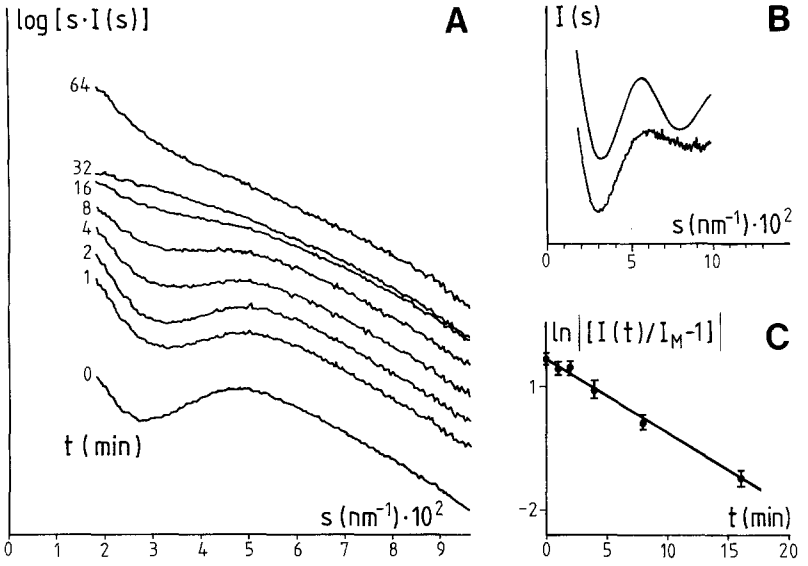

Fig. 1. **A**, X-ray scattering patterns of chicken erythrocyte chromatin (3 mg DNA/ml) after various times of digestion with micrococcal nuclease. **B**, *bottom*: Experimental interference function obtained from the ratio of the scattering patterns before and after 32 min digestion. *Top*: Theoretical interference function for a fixed internucleosomal spacing of 23 nm i.e. $\sin(46\pi s)/(46\pi s)$. **C**, Decrease in the number of internucleosomal links with digestion time assuming first order kinetics. Data are taken at the first minimum of the interference function

Kinetic information on the structural changes involved can be obtained as follows. At low ionic strength chromatin fragments are extended. Neglecting the contribution of the linker DNA to the scattering (Koch et al. 1987) they can be described at low resolution as an irregular string of nucleosomes with an average internucleosomal distance d. Neglecting the effect of the relative orientation of the nucleosomes, the scattering of such a polydisperse system at any time t during enzymatic digestion can be written as:

$$I(s,t) = f^2 \sum_{k=1}^{K} k\, N_k(t) + 2f^2 \frac{\sin(2\pi s d)}{2\pi s d} \sum_{k=2}^{K} (k-1)\, N_k(t) + 2f^2 \sum_{k=3}^{K} \sum_{m=2}^{k-1} (k-m)\, N_k(t) \frac{\sin(2\pi s m d)}{2\pi s m d}, \quad (1)$$

where f is the transform of a mononucleosome, k the degree of polymerisation, which can take values between 1 and K, and $N_k(t)$ is the number of k-mers in solution. Thus, $\sum_{k=1}^{K} k\, N_k(t)$ is the total (constant) number of nucleosomes in solution and $\sum_{k=2}^{K} (k-1)\, N_k(t)$ is the total (decreasing) number of links between nucleosomes. The last term in Eq. (1) involving longer range interactions can be neglected in a first approximation at least in the range $0.03\,\mathrm{nm}^{-1} < s < 0.06\,\mathrm{nm}^{-1}$ where the nearest neighbour contributions dominate. The second term which determines the amplitude of the interference maxima is a direct measure of the number of internucleosomal links in solution. The interference function can be extracted in a straightforward manner from the ratio of the scattering pattern at time t and that of mononucleosomes ($I_M(s)$). As an approximation, the scattering pattern obtained after 32 min can be used for this purpose (i.e. $I_M(s) = I(s, t = 32)$). Scattering patterns corresponding to longer digestion times are not usable because of the presence of aggregated material. The pattern at $t = 32$ min arises essentially from mono- to pentanucleosomes, as shown by the size distributions obtained by DNA gel electrophoresis illustrated in Fig. 2. The distributions at the various times are plotted on a linear scale rather than on the logarithmic scale of the electrophoresis gels. The use of the pattern of short oligonucleosomes is also justified because it is known from electric dichroism (Marion et al. 1981) that these do not present a superstructure. An alternative approach would have been to use the pattern of a pure mononucleosome preparation. This would have had the advantage of suppressing any remaining internucleosomal correlations, but the disadvantage of not keeping the scattering mass constant by eliminating the free DNA segments and histones.

The interference function obtained in this manner is illustrated in Fig. 1 B. Since the first minimum of $\sin 2\pi x/2\pi x$ occurs at $x = 0.7$ and the first maximum at $x = 1.4$ one can directly estimate the average internucleosomal distance to be 23 nm for this preparation. The value of

$$\left| \frac{I(s,t)}{I_M(s)} - 1 \right|$$

is thus proportional to the number of internucleosomal links. Assuming that micrococcal nuclease cuts randomly and that the reaction follows first order kinetics, the standard expressions for polymer degradation (Jungers et al. 1958) can be applied, at least in the early stages of digestion. The decrease of the interference amplitude can thus be described by the follow-

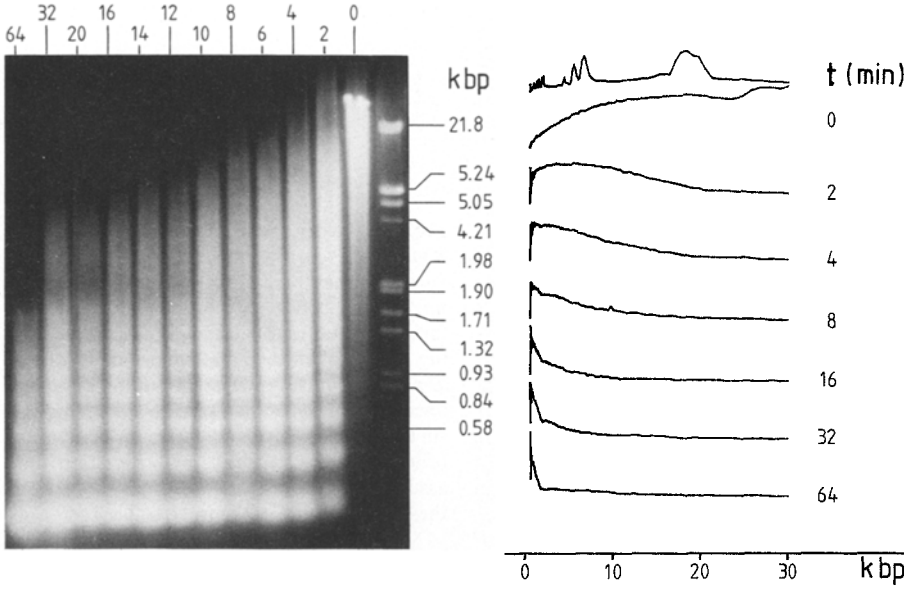

Fig. 2. DNA size distribution after different digestion times (1% agarose gel). Digestion was carried out in identical conditions as for the scattering experiments. The densitometer traces are displayed on a linear scale to present the size distribution, rather than on the logarithmic size scale of the electrophoresis gel. The markers are ECO RI plus Hind III restriction fragments of phage λ DNA

ing expression

$$\ln\left(\left|\frac{I(s,t)}{I_M(s)}-1\right|\right)=\ln\left(\left|\frac{I(s,o)}{I_M(s)}-1\right|\right)-k\,t\,.$$

As shown in Fig. 1 C this interpretation is in good agreement with the experimental data taken in the vicinity of the first minimum of the interference function.

Thermal denaturation of chromatin fragments

The evolution of the scattering curve from solutions of chicken erythrocyte chromatin fragments during thermal denaturation is shown in Fig. 3 A. The distribution of internucleosomal distances broadens and the average internucleosomal distance increases, resulting in a progressive shift of the 0.05 nm^{-1} band to smaller angles and a decrease of its intensity at higher temperatures. Similar observations were made on rat liver chromatin fragments.

The complexity of the denaturation phenomenon at low ionic strength is best illustrated by the correlation plot in Fig. 3 B in which the integrated intensity in the trough (region I: $2.75 \cdot 10^{-2} < s < 3.30 \cdot 10^{-2}$ nm^{-1}) is plotted against that near the maximum of the 0.05 nm^{-1} band (region II: $4.65 \cdot 10^{-2} < s < 5.20 \cdot 10^{-2}$ nm^{-1}) for the different temperatures. Each change of slope in the correlation plot indicates the onset of a new transition. In the straight parts, the state of the solution can be described as a linear combination of the initial and final states defined by the ends of the linear segment (Moody et al. 1980). Transitions occurring simultaneously cannot be distinguished by this method and yield a continuous straight correlation plot.

Thus, point A corresponds to the onset of the shift of the 0.05 nm^{-1} band to smaller s-values which occurs around 40 °C. Extrapolation of the scattering patterns to $s = 0$ indicates the progressive decrease of the mass per unit length and of the radius of gyration of the cross-section up to about 60 °C. Around 62 °C (point B) irreversible denaturation sets in, leading to a large increase in scattered intensity at low s-values. The corresponding correlation plot for chromatin in a buffer containing 2 mM $MgCl_2$, in the temperature range 20 to 60 °C, yields a straight line indicating a simple transition or superimposed transitions.

Optical thermal denaturation profiles were obtained from dilute samples ($A_{260} = 1.4$) by monitoring the changes in absorbance at 260 nm as illustrated in Fig. 4. Whereas the absorbance curves of chicken erythrocyte chromatin-EDTA display a small shoulder near 75 °C, those of rat liver chromatin-EDTA are monophasic with Tm = 80 °C as also observed by Marion et al. (1985).

Radiation damage

During the thermal denaturation experiments the chromatin samples were exposed to the intense X-ray beam for periods of about 30 min. To verify that the observed effects were not due to radiation damage, chromatin solutions (3 mg DNA/ml) were irradiated at different temperatures between 15 and 40 °C for periods of up to 90 min corresponding to an estimated dose of 2 M rad (Boulin et al. 1982). Changes of about 5% of the 0.05 nm^{-1} band, such as those occurring before point A in Fig. 3 B, were observed but these non systematic effects most probably only reflect changes

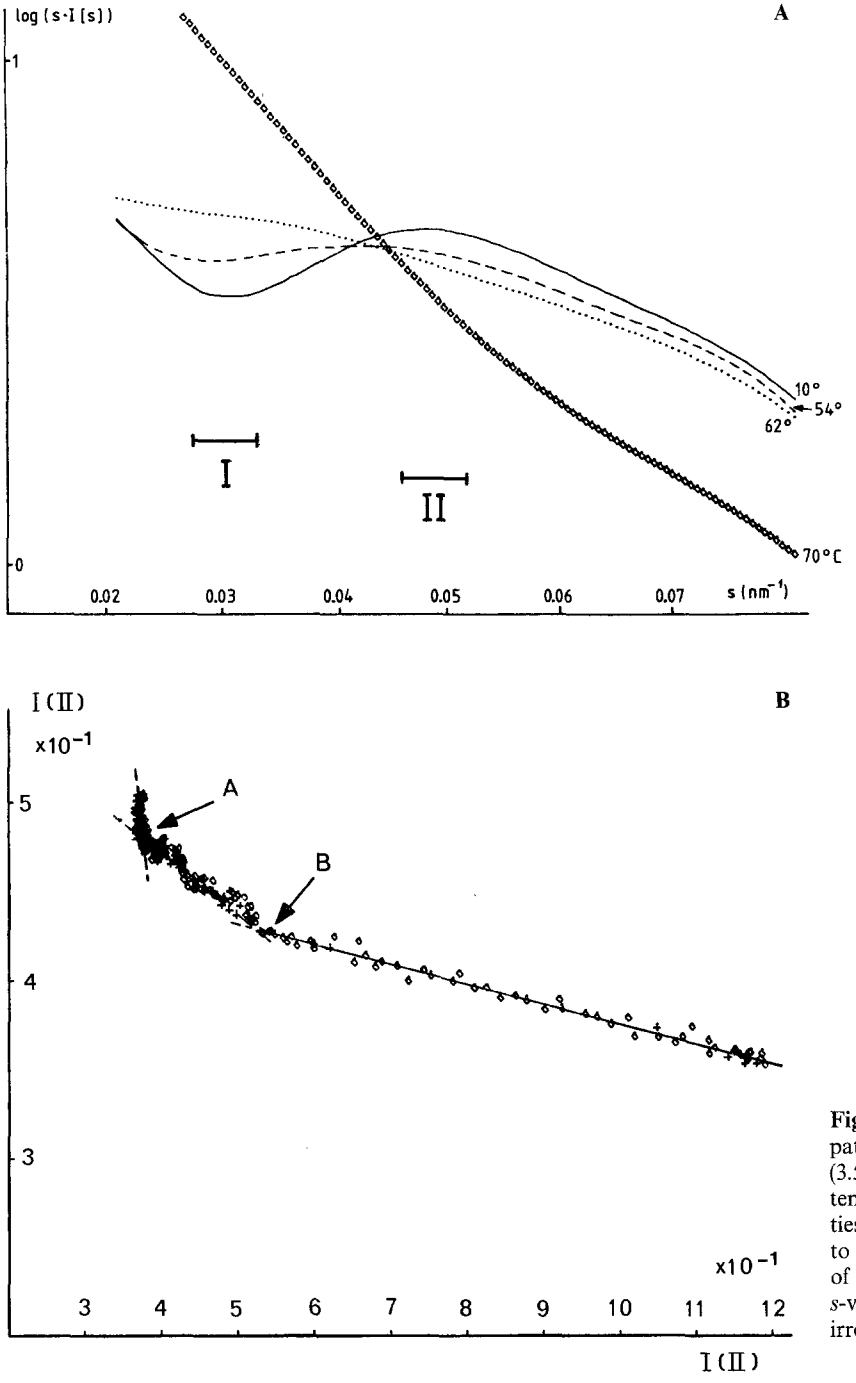

Fig. 3. **A** Evolution of the solution scattering pattern of chicken erythrocyte chromatin (3.5 mg DNA/ml) in TE buffer as a function of temperature. **B** Correlation plot of the intensities in region I and II in A. *Point A* corresponds to a temperature of about 42 °C and the onset of the shift of the 0.05 nm^{-1} band to lower *s*-values. *Point B* corresponds to the onset of irreversible denaturation at about 62 °C

of the X-ray beam during the first 20 min of the experiment.

Binding of distamycin and netropsin

Figure 5 A illustrates the broadening and shift of the 0.05 nm^{-1} band to lower *s*-values at increasing Distamycin concentrations in TE buffer. Similar behaviour is observed with Netropsin. The internucleosomal distance estimated from the position of the minima and maxima of the interference function, as explained above for the digestion experiments, increases by about 12% at 10 Dst/100 bp and by about 20% at 20 Dst/100 bp. There is a corresponding decrease of the radius of gyration of the cross-section and of the mass per unit length as shown in Fig. 5 B, which also illustrates that the effects depend on the state of condensation of the chromatin fibres. At 20 m*M* NaCl the mass per unit length increases slightly with Distamycin concentration. Distamycin at concentration levels of 5 or 10 Dst/100 bp does not prevent condensation

by NaCl. Up to about 5 Dst/100 bp $\sqrt{I(0)}$ increases linearly with NaCl concentration, with a slope similar to that observed in the absence of Distamycin (Koch et al. 1987). At higher Distamycin concentration a less compact structure appears to be formed at a given salt concentration as shown in Fig. 5C.

Discussion

The results of the digestion experiment provide unequivocal evidence that the 0.05 nm^{-1} band is due to internucleosomal interference. They provide a further argument in favour of the existence of a three dimensional zig-zag (Thoma et al. 1979) or loose helix-like structure (Bordas et al. 1986b) or irregular chain of nucleosomes with a narrow distribution of internucleosomal distances (Koch et al. 1987) in solution at low ionic strength. A jointed filament model as proposed by Greulich et al. (1987) following the approach of Kirste and Oberthuer (1982) for synthetic polymers, can give satisfactory agreement with the experimental data provided the average length of the segments is fixed at 20 – 23 nm. The model is then equivalent to that of the irregular chain (Koch et al. 1987). The results of the digestion experiments also allow us to refute the suggestion (Widom 1986) that the 0.05 nm^{-1} band may arise from intermolecular correlations of entangled 10 nm nucleosome filaments. The latter would be expected to give rise to a maximum at 0.1 nm^{-1} rather than at 0.05 nm^{-1}. Absence of the 0.05 nm^{-1} band, as in the early observations of Sperling and Tardieu (1976), can be taken as an indication for a distribution of short fragments, with less than 10 – 15 nucleosomes, in the sample. The slope of the cross-section plots is then mainly determined by the transform of the nucleosomes (Koch et al. 1987) and yields values of the cross-section radius of gyration in the range 2.8 – 3.8 nm. These findings justify the use of the 0.05 nm^{-1} band as a marker to monitor structural changes affecting the internucleosomal distance distribution in chromatin.

A first example is provided by the interaction of chromatin with Netropsin and Distamycin. Our observations are in agreement with the electron microscopy results of Lang et al. (1979) indicating a progressive extension of the fibres. The broadening of the interference band at 0.05 nm^{-1} reflects that of the distribution of internucleosomal distances. At high concentrations (> 20 mol/100 bp) denaturation occurs.

The effect of Distamycin and Netropsin on the structure of DNA depends on ionic strength. A con-

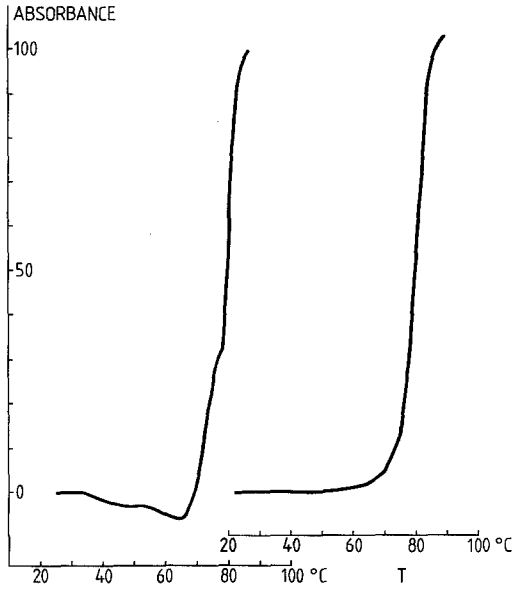

Fig. 4. Changes in absorbance for solutions (0.070 mg DNA/ml) of chicken erythrocyte (*left*) and rat liver (*right*) chromatin

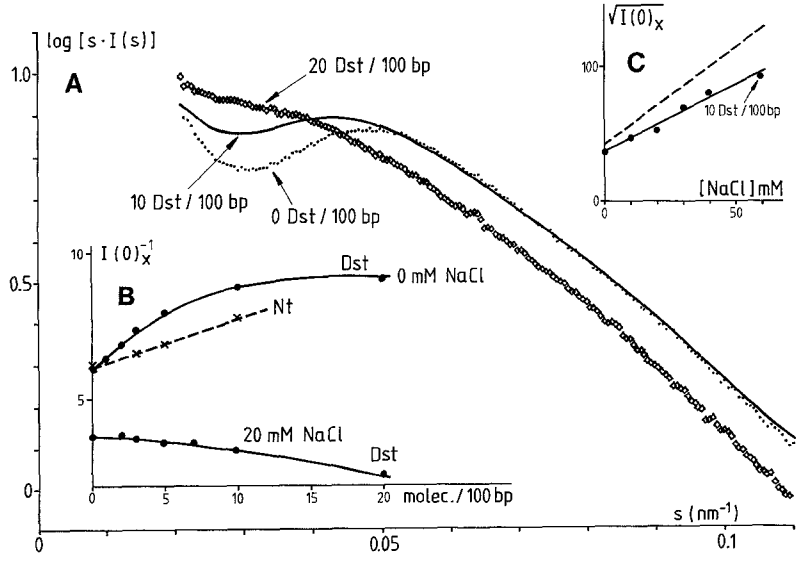

Fig. 5. **A** Scattering pattern of chicken erythrocyte chromatin in TE buffer in the presence of increasing amounts of Distamycin (*Dst*). **B** Changes of $I(0)_x^{-1}$ at increasing Netropsin (*Nt*) and Distamycin concentrations in TE buffer and in the presence of 20 m*M* NaCl. **C** Change in $\sqrt{I(0)_x}$ with NaCl concentration at a fixed concentration ratio of 10 Dst/100 bp. The *dashed line* corresponds to the effect of NaCl in the absence of Distamycin

tour length increase of about 10% at 10 Dst/100 bp was obtained by electric dichroism studies of Distamycin-DNA interaction at 2.5 m*M* Na^+ (Hogan et al. 1979). Viscosity measurements on DNA at 0.15 *M* Na^+ show, in contrast, that at the concentration ratios used in our case, Netropsin increases viscosity (Reinert 1972), except for DNA with a low $A + T$ content (Zimmer et al. 1971) whereas Distamycin decreases it. It was concluded that the effects are mainly due to a decrease in persistence length in the case of Distamycin and to the opposite effect for Netropsin (Reinert 1972, 1981) rather than to changes in the contour length.

Although it should be taken into account that effects observed on DNA may not be directly transposable to chromatin, where other structural constraints, such as those due to the nucleosomes, play a role, similar differences appear to exist for chromatin. Increasing concentrations of both Distamycin and Netropsin in the range from 0 to 10 mol/100 bp in TE buffer, lead to a decrease of the mass per unit length of chromatin. This effect is expected to lead to an increase in viscosity. At 20 m*M* NaCl, however, Distamycin appears to increase the mass per unit length very slightly probably due to neutralization of charges leading to further condensation. This should result in a decrease in viscosity.

Measurements of the internucleosomal distance do not distinguish between changes in contour length and persistence length. The experimental value of the internucleosomal distance (23 nm) suggests, however, that the linker is stiff in TE buffer. Assuming that the observed effects are mainly due to an increase in contour length of the linker, one can obtain an upper limit for the elongation per Distamycin molecule. If there is no preferential binding to linker DNA, the elongation can be estimated to be around 0.2 nm per Distamycin molecule, in satisfactory agreement with the results of Reinert (1972) for Netropsin (0.15 nm) but considerably less than the exceptionally large value reported by Hogan et al. (1979) for Distamycin and calf thymus DNA (1.3 nm). The increase in internucleosomal distance is also consistent with the results of Sen and Crothers (1986b) who found by electric dichroism that, in the absence of salt, Distamycin does not compact nor aggregate chromatin, but that there must be increased torsional or bending stiffness of the drug bound DNA. At increasing Mg^{++} concentrations they find that Distamycin does not prevent initial aggregation but is an obstacle for further folding at high Distamycin/bp ratios. This should result as shown in Fig. 5C in a lower mass/unit length than in the absence of Distamycin at a given salt concentration.

Thermal denaturation of chicken erythrocyte chromatin is associated with three transitions as determined by the change in hyperchromicity (Fulmer and Fasman 1979; Ausio et al. 1986). The first (I), reversible, salt concentration dependent transition with onset between 40° and 50 °C and midpoint in the range 55 – 65 °C is usually associated with melting of the linker. The second transition (II) with onset at 60 °C and midpoint around 70 °C, is associated with melting of the DNA region between the linker and core DNA. Melting of the core DNA corresponds to the third transition (III) with midpoint at 80 °C. The latter two transitions are also observed in the melting profiles of nucleosome cores at low ionic strength (McGhee and Felsenfeld 1980; Walker and Wolffe 1984). We observe the onset of transition I at about 40 °C. The shift of the 0.05 nm^{-1} band to lower *s*-values up to 60 °C provides a direct structural observation of the increase in internucleosomal spacing due to the melting of parts of the linker DNA. Transitions II and III, which result in the collapse of the loose helix-like structure and irreversible denaturation of the chromatin fibres, are not separated in our observations.

The superposition of transitions I and II (II + III in this case), at higher ionic strength (Fulmer and Fasman 1979) is confirmed by the correlation plot for partly condensed chromatin which yields a straight line (not shown).

In the case of rat liver chromatin, the optical thermal denaturation profile appear to be monophasic, as also observed by Marion et al. (1985), and the transitions are less distinctly separated in X-ray scattering. Thus, it seems that the observed differences have to be attributed to genuine differences in properties of chromatin from these two sources, rather than to preparative artefacts.

The two examples above show that the 0.05 nm^{-1} band is useful for monitoring changes in the state of chromatin fibers at low ionic strength, induced by external factors. This can be done in dilute solutions as well as in gels (Bordas et al. 1986a). The position and intensity of this band should also be sensitive to intrinsic structural variations. Thus, one would expect it to shift to lower *s*-values and to increase in intensity for chromatin with very long linker or on the contrary to shift to larger *s*-values and be less intense in chromatin with very short linker.

References

Ausio J, Borochov M, Seger D, Eisenberg H (1984) Interaction of chromatin with NaCl and $MgCl_2$. J Mol Biol 177: 373–398

Ausio J, Sasi R, Fasman GD (1986) Biochemical and physiochemical characterization of chromatin fractions with different degrees of solubility isolated from chicken erythrocyte nuclei. Biochemistry 25:1981–1988

Bordas J, Perez-Grau L, Koch MHJ, Nave C, Vega MC (1986a) The superstructure of chromatin and its condensation mechanism: I Synchrotron radiation X-ray scattering results. Eur J Biophys 13:157–174

Bordas J, Perez-Grau L, Koch MHJ, Nave C, Vega MC (1986b) The superstructure of chromatin and its condensation mechanism: II Theoretical analysis of the X-ray scattering patterns and model calculations. Eur J Biophys 13:175–186

Boulin C, Dainton D, Dorrington E, Elsner G, Gabriel A, Bordas J, Koch MHJ (1982) Systems for time resolved X-ray measurements using one-dimensional and two-dimensional detectors. Nucl Instrum Methods 201:209–220

Boulin C, Kempf R, Koch MHJ, McLaughlin SM (1986) Data appraisal, evaluation and display for synchrotron radiation experiments: hardware and software. Nucl Instrum Methods A249:399–407

Finch JT, Klug A (1976) Solenoidal model for superstructure in chromatin. Proc Natl Acad Sci USA 73:1879–1901

Fulmer AW, Fasman GD (1979) Ionic strength-dependent conformational transitions of chromatin. Circular dichroism and thermal denaturation studies. Biopolymers 18:2875–2891

Greulich KO, Wachtel E, Ausio J, Seger D, Eisenberg H (1987) Transition of chromatin from the "10 nm" lower order structure, to the "30 nm" higher order structure, as followed by small angle X-ray scattering. J Mol Biol 193:709–721

Hogan M, Dattagupta N, Crothers DM (1979) Transmission of allosteric effects in DNA. Nature 278:521–524

Jungers JC, Balaceanu JC, Coussement JC, Eschard F, Giraud A, Hellin M, Leprince P, Limido GE (1958) Cinetique chimique appliquee. Technip, Paris, pp 674–676

Kirste RG, Oberthuer RC (1982) In: Glatter O, Kratky O (eds) Small angle scattering. Academic Press, New York, pp 387–431

Koch MHJ, Bordas J (1983) X-ray diffraction and scattering on disordered systems using synchrotron radiation. Nucl Instrum Methods 208:461–469

Koch MHJ, Vega MC, Sayers Z, Michon AM (1987) The superstructure of chromatin and its condensation mechanism. III: Effect of monovalent and divalent cations, X-ray solution scattering and hydrodynamic studies. Eur J Biophys 14: 307–319

Lang H, Vengerov YY, Popenko VI, Zimmer Ch (1979) Structural transitions of chromatin induced by netropsin. Acta Biol Med Germ 38:33–40

Lewin B (1980) In: Gene expression, vol 2. John Wiley, New York

Marion C, Bezot P, Hesse-Bezot C, Roux B, Bernengo JC (1981) Conformation of chromatin oligomers: a new argument for a change with the hexanucleosome. Eur J Biochem 120:169–176

Marion C, Hesse-Bezot C, Bezot P, Marion M-J, Roux B, Bernengo JC (1985) The effect of histone H1 on the compaction of oligo nucleosomes. A quasi-elastic light scattering study. Biophys Chem 22:53–64

McGhee JD, Felsenfeld G (1980) The number of charge-charge interactions stabilizing the ends of nucleosome DNA. Nucleic Acids Res 8:2751–2769

Moody MF, Vachette P, Foote AM, Tardieu AM, Koch MHJ, Bordas J (1980) Stopped-flow X-ray solution scattering: the dissociation of Aspartate transcarbamylase. Proc Natl Acad Sci USA 77:4040–4043

Perez-Grau L, Bordas J, Koch MHJ (1984) Synchrotron radiation X-ray scattering study on solutions and gels. Nucleic Acids Res 12:2987–2995

Reinert KE (1972) Adenosine. Thymidine cluster-specific elongation and stiffening of DNA induced by the oligopeptide antibiotic Netropsin. J Mol Biol 72:593–607

Reinert KE (1981) Aspects of specific DNA-protein interaction; local bending of DNA molecules by in-register binding of the oligopeptide antibiotic Distamycin. Biophys Chem 13:1–14

Sen D, Crothers DM (1986a) Condensation of chromatin: role of multivalent cations. Biochemistry 25:1495–1503

Sen D, Crothers DM (1986b) Influence of DNA-binding drugs on chromatin condensation. Biochemistry 25:1503–1509

Sperling L, Tardieu A (1976) The mass per unit length of chromatin by low angle X-ray scattering. FEBS Lett 64:89–91

Thoma F, Koller T, Klug A (1979) Involvement of histone H1 in the organization of the nucleosome and of the salt dependent superstructures of chromatin. J Cell Biol 83:403–427

Walker IO, Wolffe AP (1984) The thermal denaturation of chromatin core particles. Biochim Biophys Acta 785:97–103

Widom J (1986) Physicochemical studies of the folding of the 100 Å nucleosome filament into the 300 Å filament. J Mol Biol 190:411–424

Yaniv M, Cereghini S (1986) Structure of transcriptionally active chromatin. CRC Crit Rev Biochem 21:1–26

Zimmer Ch, Wahnert U (1986) Nonintercalating DNA-binding ligands: specificity of the interaction and their use as tools in biophysical, biochemical and biological investigations of the genetic material. Prog Biophys Mol Biol 47:31–112

Zimmer Ch, Reinert KE, Luck G, Wahnert U, Lober G, Thrum H (1971) Interaction of the oligopeptide antibiotics Netropsin and Distamycin A with nucleic acids. J Mol Biol 58:329–348